

# In Vitro Tendon Models to Investigate the Effect of Matrix Microarchitecture on Extracellular Vesicle Profile

Kariman Shama<sup>1</sup>, Zachary Greenberg<sup>3</sup>, Kathrina Etienne<sup>2</sup>, Mei He PhD<sup>3</sup>, Brittany Taylor PhD<sup>1</sup>

<sup>1</sup>J. Crayton Pruitt Family Department of Biomedical Engineering, University of Florida, Gainesville, Florida, <sup>2</sup>University of Pittsburgh School of Medicine Physical Medicine and Rehabilitation <sup>3</sup>Department of Pharmaceutics, College of Pharmacy, University of Florida, Gainesville, Florida

[k.shama@ufl.edu](mailto:k.shama@ufl.edu)

**Disclosures:** KS (N), ZG (N), KE (N), MH (N), BT (N).

**INTRODUCTION:** Tendon healing's intricate cellular communication employs extracellular vesicles as mediators, conveying bioactive molecules for the multiple stages of healing. Mesenchymal stem cell derived extracellular vesicles (EVs) play a role in the cell-to-cell communication throughout the tissue healing process by exchanging information between the cells in the injured tissue microenvironment<sup>1</sup>. EVs are membrane-bound vesicles that transport biomolecules to cells; their role in tendon pathology, immunomodulation, and healing remains incompletely understood, potentially holding insights into mechanisms underlying inadequate tendon healing<sup>2</sup>. To understand the different roles and characteristics of EVs in various tendon healing microenvironments, we fabricated highly aligned and unaligned polycaprolactone (PCL) electrospun scaffolds with varying fiber densities to mimic disorganized pathologic and healthy tendinous tissue, respectively. We therefore aim to characterize EVs within our in vitro tendon models by observing differences in EV concentration, EV marker expression and yield per metabolically active cell within the different microenvironments. Our hypothesis posits that EV secretion profiles will correlate with the tissue microenvironment, wherein stiffer unaligned scaffolds will result in heightened EV secretion, an elevated EV secretion per metabolically active cell, and enhanced CD9 expression.

**METHODS:** To determine the effect of scaffold density and alignment on EV secretion, 50% w/v and 75% w/v PCL scaffolds were electrospun onto a mandrel rotating at approximately 100 and 800 RPM to create unaligned and aligned nanofibrous scaffolds, respectively. Scanning electron microscopy (SEM) and ImageJ were performed to analyze fiber alignment and diameter, and matrix morphology. Scaffolds were seeded with NIH3T3 fibroblasts at a density of  $1 \times 10^6$  cells/scaffold. EVs were isolated from culture media using a qEV 70 nm columns (IZON Science) after 1, 3, 5, and 7 days of cell culture. Nanoparticle tracking analysis (NTA) was performed to assess EV size distribution and concentration. Total protein content was assessed by Bicinchoninic Acid (BCA) assay for EV purity and to determine CD9, CD63, CD81, TSG101, and calnexin expression via Western blot. An MTS Tetrazolium Assay to assess metabolic activity of the cells. Tensile mechanical testing was performed on scaffolds utilizing a ramp-to-failure protocol of 18% strain/min. One-way ANOVAs with multiple comparisons were used to evaluate scaffold properties and fiber diameter; a two-way ANOVA with multiple comparisons assessed EV changes over time, while nonparametric one-way ANOVA analyzed fibril alignment ( $p < 0.05$ ).

**RESULTS:** SEM analysis demonstrated PCL constructs had significant variation in alignment, with the 75% w/v group having an overall higher alignment than the 50% w/v group (Fig. 1, 2A). Significantly varied fibril diameter was also displayed, with the 75% w/v 100 RPM group and 50% w/v 800 RPM group displaying the thickest and thinnest fibers, respectively (Fig. 2B). The scaffold with 75% w/v concentration at 100 RPM exhibited the highest Young's Modulus ( $221.4 \pm 39.26$  MPa) and UTS ( $2.320 \pm 1.041$  MPa) compared to other scaffolds (Fig. 2C,D). All scaffolds demonstrated significantly distinct Young's Moduli and UTS values, except for the 75% w/v 800 RPM and 50% w/v 800 RPM, which had similar Young's Moduli ( $57.29 \pm 7.671$  MPa and  $52.95 \pm 18.11$  MPa, respectively) and UTS ( $1.130 \pm 0.2261$  MPa and  $1.379 \pm 0.3615$  MPa, respectively). MTS and NTA analysis demonstrate no significant difference in EV secretion normalized to metabolically active cells. NTA revealed a significant increase in EV secretion in the 50% w/v 100 RPM scaffold from day 1 to 5, and on day 3, EV secretion significantly increased in the same scaffold group compared to TCP (Fig. 3).

**DISCUSSION:** Our objective was to create in vitro tendinopathy models, investigating the impact of microarchitecture on extracellular vesicle (EV) secretion. Notably, aligned nanofibrous scaffolds have shown the ability to mechanically and morphologically stimulate mesenchymal stem cells (MSCs)<sup>3</sup>. Furthermore, it has been observed that 3D hydrogel-cultured MSC-derived EVs yield a significantly higher quantity of EVs<sup>4</sup>. In light of these findings, we aimed to combine these aspects by examining how microarchitecture influences EV secretion in our fabricated tendinopathy models. Scaffold fiber diameters are within the range of native collagen fibers ( $1-20 \mu\text{m}$ )<sup>6</sup>. Furthermore, the Young's Moduli of the PCL nanofibrous scaffolds were on the lower end of native tendon tensile properties ( $20-1000$  MPa)<sup>7</sup>. The 75% w/v 100 RPM group had the largest fiber diameters and highest tensile properties. Larger diameter fibers are more phenotypically conducive to pathologic microenvironments in the latter stages of tendon healing<sup>8</sup>. Additionally, cells have been shown to produce higher secretions of EVs on stiffer biomaterials<sup>9</sup>. This was not demonstrated by the data shown, as there is a significant time dependent increase for the 50% w/v 100 RPM group between days 1 and 3. Additionally, the same group on day 3 demonstrated an upscale EV secretion compared to the TCP control. This observation is consistent with literature on scaling up EV-stimulation in three-dimensional culture systems, as well as biophysical stimulation resulting from electrospun nanofibers<sup>10-12</sup>. Western blot analysis (*data not shown*) demonstrated low detection of bands for all markers. This is most likely attributed to the isolation technique utilized, as literature indicates poor detection of markers CD9, CD63, CD81, TSG101 and EV-exclusion marker calnexin with qEV size exclusion columns<sup>13, 14</sup>. Future work entails utilizing different EV isolation methods such as ultracentrifugation.

**SIGNIFICANCE/CLINICAL:** Current tendinopathy treatments lack in targeting the etiology of disease; EVs offer cell-free tendon healing, overcoming cellular therapy limitations. The current research enhances understanding of EV-mediated cell communication's role in healthy and pathologic microenvironments, offering insights into EVs as potential biomarkers and treatments for tendinopathies.

**REFERENCES:** 1. Chen SA-O, Int J Mol Sci. 2021. 2. Doyle LM, Cells. 2019. 3. Qiu Y, J Tissue Eng Regen Med. 2016. 4. Kim M, Yun HW, Tissue Eng Regen Med. 2018. 5. Seth A, Ty M, Journal of Immunol. and Reg. Med. 2020. 6. Calejo I, Adv Health Mater. 2022. 7. LaCroix AS, J Appl Physiol. 1985. 8. Birk DE, Eur J Cell Biol. 1997. 9. Patwardhan S, Biomaterials. 2021. 10. Ng CY, Int J Mol Sci. 2022. 11. Thippabhotla S, Sci Rep. 2019. 12. Erwin N, Pharm Res. 2023. 13. Brennan K, Sci Rep. 2020. 14. Stranska RA-OX, J Transl Med. 2018.

**ACKNOWLEDGEMENTS:** This work was supported in part by the University of Florida Provost's Office of Research and the Alliance for Regenerative Rehabilitation Research and Training (AR<sup>3</sup>T) pilot grant.

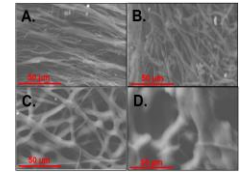


**Figure 1:** SEM images of PCL scaffolds: 50% w/v (A) at 800 RPM and (B) 100 RPM, and 75% w/v at (C) 800 RPM, (D) 100 RPM (1000x).

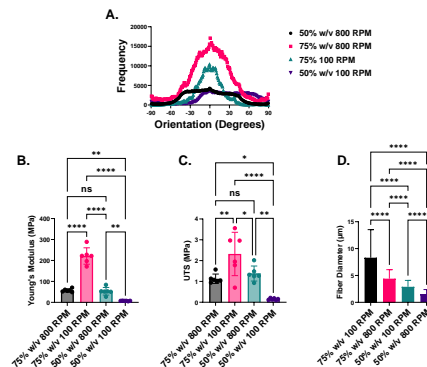


**Figure 2:** (A) Fiber orientation analysis demonstrated the 75% w/v 800 RPM scaffold had the highest alignment (pink line). (B) Fiber diameter, (C) Young's modulus, and (D) Ultimate tensile strength was significantly influenced by the polymer density and fiber orientation. (\*) indicates  $p < 0.05$ , (\*\*) indicates  $p < 0.01$ , (\*\*\*) indicates  $p < 0.001$ .

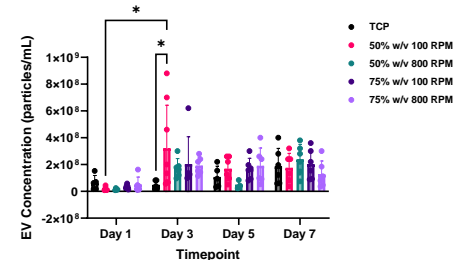


**Figure 3:** EV secretion analyzed via NTA was influenced by the scaffold's microarchitecture over time. (\*) indicates  $p < 0.05$ .